Bioactive Materials 13 (2022) 212–222

Contents lists available at ScienceDirect

Bioactive Materials

journal homepage: www.keaipublishing.com/en/journals/bioactive-materials

De novo strategy with engineering a multifunctional bacterial cellulose-based dressing for rapid healing of infected wounds

Chen Zhou [a], Zhifei Yang [a], Xiaowei Xun [a], Le Ma [a], Zejing Chen [a], Xiaoming Hu [a], Xidong Wu [b], Yizao Wan [a,**], Haiyong Ao [a,*]

[a] Jiangxi Key Laboratory of Nanobiomaterials & Institute of Advanced Materials, East China Jiaotong University, Nanchang, 330000, China
[b] Department of Drug Safety Evaluation, Jiangxi Testing Center of Medical Device, Nanchang, 330000, China

ARTICLE INFO

Keywords:
Bacterial cellulose
Quaternized chitosan
Multifunctional dressing
Antibacterial activity
Healing promotion

ABSTRACT

The treatment and healing of infected skin lesions is one of the major challenges in surgery. To solve this problem, collagen I (Col-I) and the antibacterial agent hydroxypropyltrimethyl ammonium chloride chitosan (HACC) were composited into the bacterial cellulose (BC) three-dimensional network structure by a novel membrane–liquid interface (MLI) culture, and a Col-I/HACC/BC (CHBC) multifunctional dressing was designed. The water absorption rate and water vapor transmission rate of the obtained CHBC dressing were 35.78 ± 2.45 g/g and 3084 ± 56 g m^{-2}·day^{-1}, respectively. The water retention of the CHBC dressing was significantly improved compared with the BC caused by the introduced Col-I and HACC. *In vitro* results indicated that the combined advantages of HACC and Col-I confer on CHBC dressings not only have outstanding antibacterial properties against *Staphylococcus aureus* (*S. aureus*) compared with BC and CBC, but also exhibit better cytocompatibility than BC and HBC to promote the proliferation and spread of NIH3T3 cells and HUVECs. Most importantly, the results of *in vivo* animal tests demonstrated that the CHBC dressings fully promoted wound healing for 8 days and exhibited shorter healing times, especially in the case of wound infection. Excellent skin regeneration effects and higher expression levels of collagen during infection were also shown in the CHBC group. We believe that CHBC composites with favorable multifunctionality have potential applications as wound dressings to treat infected wounds.

1. Introduction

As the first protective barrier of the body, human skin is the most vulnerable organ and easily cause wounds due to various factors, such as the mechanical injury and the pathological ulcer [1]. Skin wounds have been passively protected by wound dressings for centuries. However, the skin cannot undergo self-repair when the diameter of the full-thickness skin defect is more than 4 cm [2]. More importantly, as open wounds, skin wounds are easily infected by common pathogenic bacteria, such as *Staphylococcus aureus* (*S. aureus*), and infection delays wound healing [3]. Therefore, it is necessary to develop multifunctional dressings that resist infection and promote healing as active components of the healing process.

Over the last thirty years, bacterial cellulose (BC) biosynthesized by *Acetobacter xylinum* has received considerable attention as a candidate for wound dressing due to its inherent performances, such as ultrafine three-dimensional network structure, high wet strength, excellent gas permeability, high water absorbency and favorable biocompatibility [4–7]. Compared with traditional dressings such as gauze and medical sponges, BC-based dressing changes are easy and painless and do not damage the skin. The nanofiber network structure can prevent bacterial invasion and protect the wound from infection. Favorable water absorption is helpful for removing toxins, and a satisfactory water vapor transmission rate can maintain a moist environment that is conducive to the growth of granulation [8]. Nevertheless, pure BC has neither favorable bactericidal properties nor bioactive groups to promote severe skin injury repair, which limits its application in severe wound care.

To improve the cytocompatibility of BC-based dressings, collagen [1], hyaluronic acid [9] and arginine [10,11] have been introduced into the 3D structure of BC *via* various methods. The results indicated that the

Peer review under responsibility of KeAi Communications Co., Ltd.
* Corresponding author.
** Corresponding author.
E-mail addresses: yzwantju@126.com (Y. Wan), aohaiyong@ecjtu.edu.cn (H. Ao).

https://doi.org/10.1016/j.bioactmat.2021.10.043
Received 11 August 2021; Received in revised form 26 October 2021; Accepted 28 October 2021
Available online 3 November 2021

modified BC materials exhibited good cytocompatibility, promoted the proliferation and migration of fibroblasts and endothelial cells, and showed faster tissue repair in the absence of infection. However, for open wounds, preventing infection is the top priority. The above dressing cannot be used for healing infected wounds. Several studies have focused on enhancing the antimicrobial abilities of BC-based dressings using antibacterial agents, such as silver and other inorganic nanoparticles [12–15], quaternary ammonium compounds [8], antimicrobial peptides [16], thymol [17], lignin-derived compounds [18], ketoprofen [19] and amoxicillin [20,21]. Nevertheless, most of these antibacterial agents showed strong cytotoxicity, although their slow release has been achieved by various methods [22–24]. As a chitosan derivative, hydroxypropyltrimethyl ammonium chloride chitosan (HACC) exhibits better antibacterial properties than chitosan because of the grafted cationic quaternary ammonium group and improved water solubility [25]. As a cationic antibacterial agent, HACC can destroy the cell wall of gram-positive bacteria (such as *S. aureus*) to achieve antibacterial effect. Interestingly, HACC with a moderate DS of quaternary ammonium (approximately 18–30%) exhibited evident antibacterial properties and good compatibility with osteogenic cells [26–28]. In our previous study, a HACC/BC dressing was prepared *via* in situ biosynthesis, which exhibited favorable antibacterial activities and no cytotoxicity [29]. Nevertheless, cells in the HACC/BC group had spherical morphology, as did those in the BC group, and the viability of the cells was not improved by the addition of HACC.

In our previous work, HACC was covalently immobilized layer by layer onto the surface of titanium coatings combined with collagen I (Col-I) and hyaluronic acid (HA) [30]. The results demonstrated that the good antimicrobial properties of multilayer modified titanium coatings originated from HACC, while their cytobiological performance was improved by Col-I and HA. Given this revelation, we hypothesized that if HACC and Col-I were to be introduced into the structure of BC simultaneously, a novel BC-based multifunctional wound dressing with favorable antimicrobial properties and cytocompatibility would be obtained.

The primary objective of the present study was to develop a multifunctional BC-based dressing with favorable anti-infective properties and to promote healing ability for infected wounds. The antibacterial agent HACC and bioactive material Col-I were introduced simultaneously into the 3D network structure of BC *via* a novel membrane–liquid interface (MLI) culture according to the aerobic habits of *Acetobacter xylinum*, *via* which Col-I and HACC could composite with BC uniformly layer-by-layer [31]. The obtained Col-I/HACC/BC dressings were characterized by scanning electron microscopy (SEM), X-ray diffraction (XRD) and Fourier transform infrared spectroscopy (FTIR). The porosity, thermostability, water absorptivity and water retention capacity of BC-based dressings were also investigated. *In vitro*, *S. aureus* (ATCC 25923) was used to research the antibacterial activities of the obtained dressings, while NIH-3T3 and HUVECs were employed to evaluate the cytocompatibility of the samples. Furthermore, an infection model of total skin injury on the backs of mice was employed to appraise the ability of the dressings to address infection trauma.

2. Materials and methods

2.1. Materials

Col-I from pigskin with a molecular weight of 3.0×10^5 Da was purchased from Sichuan Minglet Biological Technology Co., Ltd. Chitosan (CS) with a molecular weight of 8.0×10^4 Da was provided by Zhejiang Aoxing Biotechnology Co., Ltd. Glycidyl trimethyl ammonium chloride (GTMAC) was purchased from Shanghai Macklin Biochemical Co., Ltd. HACC with a moderate degree of substitution (DS, 22%) of quaternary ammonium was prepared by grafting GTMAC to CS as previously reported [25].

2.2. Preparation of the Col-I/HACC/BC multifunctional dressing

The Col-I/HACC/BC multifunctional dressing was prepared by MLI culture, as described in the literature [32]. Briefly, 400 μL culture medium and 100 μL seed solution of *Acetobacter xylinum* were added to 24-well dishes and incubated for 3 d to prepare a pure BC pellicle (approximately 200 μm thick) as the substrate membrane. Then, 100 μL culture medium with 1 mg/mL Col-I and 3 mg/mL HACC was sprayed onto the substrate in a mist to form a membrane-liquid interface on the substrate, and BC was grown until the membrane-liquid interface was completely consumed in 2 h. Twenty cycles of spraying were performed until a predetermined BC-based composite thickness (approximately 2 mm) was obtained. After removing the substrate membrane, samples were purified by ultrasonic cleaning in deionized water and freeze-dried. The obtained Col-I/HACC/BC composite dressing was named CHBC (Fig. 1).

The Col-I/BC (denoted as CBC) and HACC/BC (denoted as HBC) composite dressings were fabricated according to the above methods. Pure BC membranes as a control group were prepared *via* static cultivation. After counting the amount of COL-I and HACC added and weighing the dried CHBC film, the weight ratio of Col-I and HACC in BC-based films was calculated. The results were shown in Table S1.

2.3. Characterization

After sputter coating with gold, the surface morphologies of samples were observed by SEM (SU8010, Hitachi, Japan). The porosities of the specimens were investigated by the liquid displacement method according to the description in our previous study [29]. The chemical compositions of the samples were analyzed by FTIR (Nicolet 6700, Thermo Electron Corporation, USA) in a spectral range of 4000–500 cm^{-1} with a resolution of 4 cm^{-1}. The phase compositions of BC-based composites were measured using XRD (D8 ADVANCE, Bruker, Germany) using Cu K_α radiation ($\lambda = 0.1541$ nm) at a scanning rate of 0.075° s^{-1} over a 2θ range of 10–30°. The crystallinity index (*C.I.*) was calculated by Segal's method [33]:

$$C.I.(\%) = \frac{I_{200} - I_{am}}{I_{200}} \times 100\% \quad (1)$$

where I_{200} is the maximum intensity (in arbitrary units) of the (200) lattice diffraction and I_{am} is the intensity of diffraction in the same units at $2\theta = 18°$.

2.4. Thermostability

Thermogravimetric analysis of the samples was performed by a Pyris 1 thermogravimetric (TG) analyzer (Diamond TG/DTA, PerkinElmer, America) with a heating rate of 10 °C min^{-1} from room temperature to 600 °C.

2.5. Water absorbency and water retention capacity

The dried specimens (weight denoted as W_{dry}) were placed in distilled water to absorb water. At certain time points, after the water on the surface of the samples was gently removed by filter paper, the specimens were weighed (weight denoted as W_{t1}). The water absorption ratio (*WAR*, %) of the specimens was calculated as follows:

$$WAR(\%) = \frac{W_{t1} - W_{dry}}{W_{dry}} \times 100\% \quad (2)$$

Samples filled with water (weight denoted as W_{wet}) were placed at room temperature, and then weighed at a given time point (W_{t2}). The water retention ratio (*WRR*, %) was calculated as follows:

$$WRR(\%) = \frac{W_{t2} - W_{dry}}{W_{wet} - W_{dry}} \times 100\% \quad (3)$$

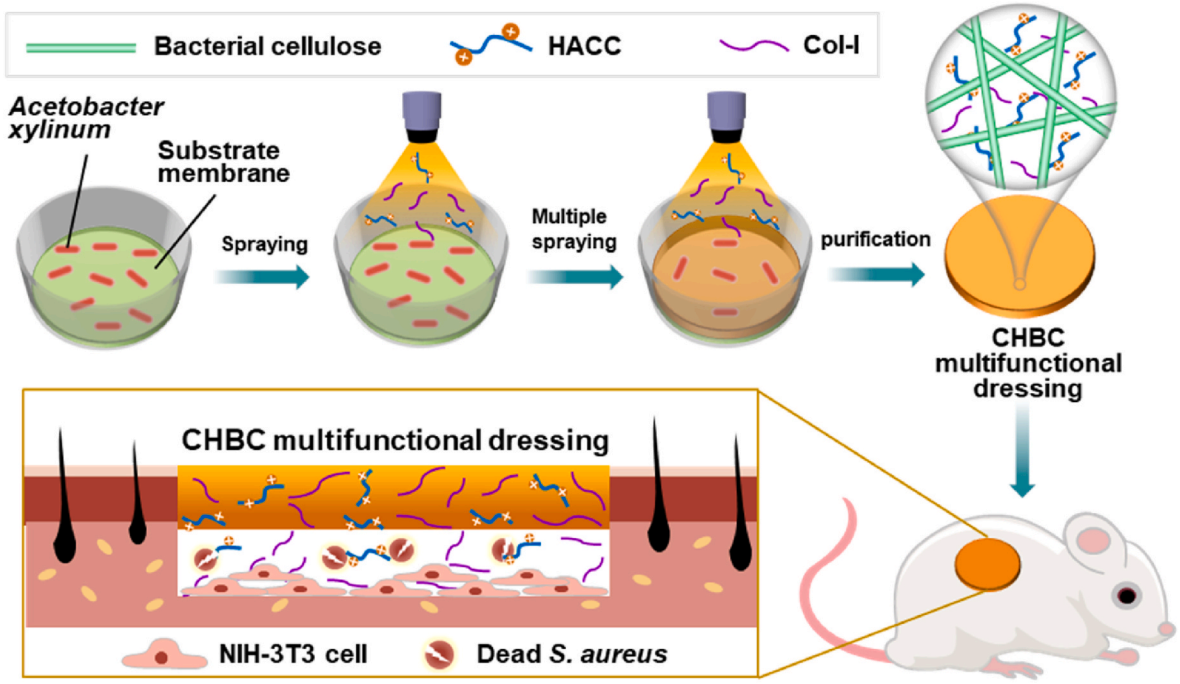

Fig. 1. Schematic illustration of the preparation of a CHBC functional dressing *via* a novel membrane–liquid interface culture and the process of treating infected wounds *in vivo*.

2.6. Water vapor transmission rate

The water vapor transmission rates (WVTRs) of the specimens were tested based on the American Society for Testing and Materials standard (ASTM E−96) as described in the literature [34]. Briefly, a 50 mL glass centrifuge tube containing anhydrous calcium chloride was sealed with the sample, and 90% relative humidity was maintained at 37 °C. The weight of the centrifuge tube was measured every day for 6 days, and the WVTR ($g \cdot m^{-2} \cdot day^{-1}$) was calculated by dividing the added mass of the centrifuge tube (Δm, g) by the cell area (A, m^2) and time (t, day).

2.7. Antibacterial properties

The zone of inhibition (ZOI) of BC-based dressings was measured by the agar plate diffusion method according to GB/T 20944 and evaluated against *S. aureus* (ATCC 25923). A bacterial turbidimetric tube obtained from Kont Bio-Chem Technology Co. (Shenzhen, China) was used to determine the concentration of bacteria. Briefly, 1×10^8 CFUs in 200 μL bacterial suspensions were evenly plated onto tryptone soy agar (TSA), and one specimen was placed on the center of the TSA and then cultivated for 24 h at 37 °C. The ZOIs were observed and their widths were measured as described in the literature [29].

To further investigate the antibacterial properties of BC-based dressings, each specimen was immersed in 1 mL of bacterial suspension containing 1×10^6 CFUs in a 24-well dish and incubated for 6 h or 24 h at 37 °C. The obtained bacterial/material samples were divided into two parts. One part was fixed in 2.5% glutaraldehyde solution, dehydrated using a series of graded ethanol solutions, and then observed through SEM (SU8010, Hitachi, Japan). The other part was stained with LIVE/DEAD BacLight Bacterial Viability kits, and then, observed by confocal laser scanning microscopy (CLSM, Leica TCS SP2, Leica Microsystems, Germany).

2.8. Cytocompatibility

NIH-3T3 cells were obtained from the Cell Bank of the Chinese Academy of Sciences and HUVECs were provided by Beijing Yuhengfeng Technology Co., LTD, which were used to investigate the cytocompatibility of BC-based dressings. Cells were cultured in DMEM culture medium (Invitrogen, Carlsbad, CA) supplemented with 10% fetal bovine serum (FBS) and 1% antibiotics at 37 °C in a humidified incubator of 5% CO_2. After sterile materials were placed in 24-well dishes, 1×10^4 cells were added and cultured for 1, 3 and 6 days. The viability of cells at each time point was tested with a CCK-8 kit according to a procedure described previously [35]. To accurately present the effects of additives on cell activity, the optical density (OD) value at day 1 was measured as a baseline, and the relative viability of cells was expressed as the ratio of the OD value relative to the value for day 1 of the same specimen.

The morphology of cells of different samples was observed by SEM and CLSM. Cells were cultured with BC-based composites for 3 days. For SEM, after fixation in 2% glutaraldehyde, specimens were dehydrated in a graded series of ethanol and ethanol/hexamethyldisilazane (HMDS) at various proportions. The cells on the specimens were observed by SEM (SU8010, Hitachi, Japan). For the CLSM assay, the cytoskeleton was stained with Alexa Fluor 555 phalloidin (Molecular Probe, Sigma–Aldrich) and the cell nuclei were stained with 4,6-diamidino-2-phenylindole (DAPI; Molecular Probe, Sigma–Aldrich), as described in the literature [36].

2.9. In vivo wound healing

All mice (Kunming mice, 8–12 weeks, provided by Model Animal Research Center of Nanjing University) were randomized into five groups and adapted to the breeding environment for 1 week. After anaesthetization through intraperitoneal injection of chloral hydrate (0.5 mg/kg body weight), a full-thickness round skin wound (Φ10 mm) was created on the back of each mouse. A total of 1×10^4 CFU *ATCC 25923* was added to the surface of the wound. The mice in the four groups were bandaged with sterilized BC, CBC, HBC and CHBC. For the control group, PBS was added to the surface of the wound, which was then bandaged with sterilized BC. The dressing films were changed every 2 days, and the contraction of the wound was measured and imaged. Surgical dressing changes were performed under aseptic conditions. The wound area recovery closure (RC) was measured by the

following formula [21]:

$$RC\ (\%)=(R_0^2-R_1^2)/R_0^2 \times 100\% \quad (4)$$

where R_0 is the width of the wound area created and R_1 is the width of the wound on the day that the wound dressing was changed.

To evaluate the histology and deposited collagen fibers of the wound tissue, mice were sacrificed at 4 days and 8 days and the wound tissues were collected in 2.5% (v/v) glutaraldehyde for 24 h. Then, each specimen was dehydrated by graded alcohols and embedded in paraffin. Five-millimeter-thick tissue sections were collected and stained with hematoxylin and eosin (H&E) and Masson's trichrome.

2.10. Statistical analysis

Experiments were repeated five times for each sample. Statistical analysis was performed with SPSS software. All data were expressed as the mean ± standard deviation. Statistical significance was determined ($P < 0.05$).

3. Results and discussion

3.1. Characterization of CHBC multifunctional dressing

Fig. 2(A) shows the SEM images of BC-based dressings. The fibers of BC were uniform and smooth, and there was much space between the fibers, as described in the literature [8]. On the SEM images of HBC, some pores of BC were filled with HACC, and the structure of BC was also obvious. In contrast, the BC fibers of CBC were conglutinated with each other by Col-I. The CHBC image showed features of both HBC and CBC, which were affected by HACC and Col-I. The structural change in BC-based composite films along with the introduction of different materials was also verified by measurement of porosity *via* the dielectric saturation method (Fig. 2(B)). The porosity of BC was 89.82 ± 1.13%. After HACC was added, the porosity of HBC decreased to 82.57 ± 1.63%, while CBC had the lowest porosity (70.68 ± 1.98%). The porosity of CHBC was 77.96 ± 1.82%, which was between that of HBC and that of CBC.

To further determine the surface chemistry of the samples, FTIR analyses of BC, HACC, Col-I, HBC, CBC and CHBC were carried out (Fig. 2(C)). BC showed O–H stretching at 3346 cm^{-1}, aliphatic C–H stretching at 2897 cm^{-1} and C–O–C stretching vibrations at 1166 cm^{-1}, 1119 cm^{-1} and 1058 cm^{-1} [37]. In the spectrum of HACC, the peak at 1648 cm^{-1} was due to amide I absorption, the peak at 1568 cm^{-1} corresponded to the deformation vibration of $–NH_2$ groups, and the peak at 1481 cm^{-1} was ascribed to C–H bending of the trimethylammonium group [25,38]. For Col-I, the peak at 1651 cm^{-1} was ascribed to the C═O stretching vibration, the peak at 1541 cm^{-1} was due to N–H bending, and the peak at 1240 cm^{-1} was attributed to the C–N stretching vibration [39]. Obviously, the FTIR curve of CHBC included all characteristic peaks of BC, HACC and Col-I, which further indicated that HACC and Col-I were successfully introduced into the BC structure. On closer inspection, the blueshift occurred at characteristic peaks of C–H stretching, C═O stretching and $–NH_2$ deformation vibration, which indicated that there were intermolecular interactions between the BC fibrils and Col-I and HACC molecules.

Fig. 2(D) shows the XRD spectra of BC, HBC, CBC and CHBC. From the XRD spectra, the XRD pattern of BC exhibited diffraction peaks at 2θ values of approximately 14.90°, 17.34° and 23.03°, which were considered to be the (11(−)0), (110), and (200) reflection planes of the cellulose I structure, respectively [40]. After introducing HACC and Col-I, the XRD patterns of HBC, CBC and CHBC did not change significantly, which means that the introduction of HACC and Col-I did not influence the crystal structure of BC. After careful observation, the three diffraction peaks of HBC, CBC and CHBC were slightly shifted. To further verify the slight changes, *C.I.* of samples were calculated. The *C.I.* of HBC, CBC and CHBC are significantly lower than that of BC. The results indicated that the presence of HACC and Col-I in the BC culture medium has an effect on the formation process of BC crystals. Similar results have been found in our other work [41,42].

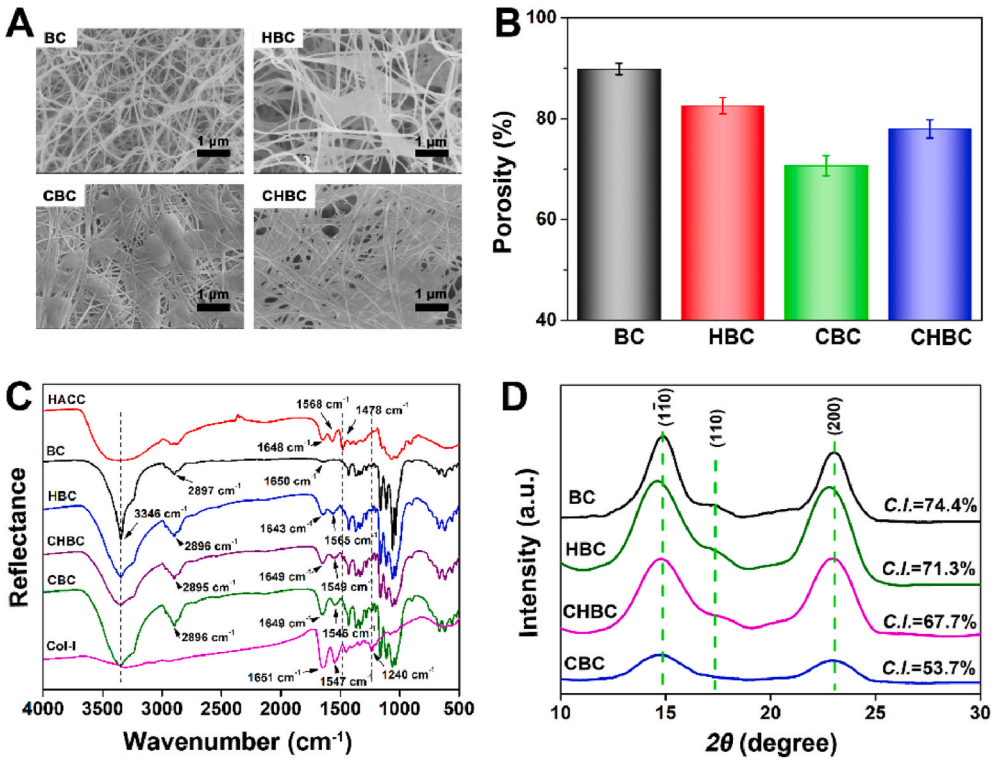

Fig. 2. Characterization of BC-based composite films. (A) SEM images of BC, HBC, CBC and CHBC; (B) porosity of BC, HBC, CBC and CHBC; (C) FTIR spectra of BC, HACC, Col-I, HBC, CBC and CHBC; (D) XRD patterns of BC, HBC, CBC and CHBC.

3.2. Thermostability

The thermostability of BC-based dressings investigated by TG analysis is shown in Fig. 3(A). Three mass loss steps were observed in the TG curves of BC: evaporation of free water at 50–100 °C with 5% weight loss, depolymerization and decomposition of BC at 313–410 °C with approximately 80% mass loss, and the carbonization process at 400–600 °C [43–45]. The excellent thermostability of BC was mainly due to its high crystallinity and purity. After introducing Col-I or HACC, the organic decomposition temperature of HBC (234–380 °C) and CBC (300–383 °C) was obviously lower than that of BC, which could be attributed to the decreased crystallinity of BC and lower thermostability of Col-I and HACC [37]. Interestingly, depolymerization and decomposition of CHBC occurred from 310 to 400 °C. In other words, the thermostability of CHBC was better than that of CBC and HBC. The reason for this may be the intermolecular interactions among Col-I, HACC and BC, which were obtained by FTIR assay. Finally, the ash content of samples was 1.7% for BC, 6.2%% for HBC, 16.2% for CBC and 17.0% for CHBC. In the derivative thermogravimetric (DTG) curve of the samples (Fig. S1), the maximum peaks of BC, CBC, HBC and CHBC occurred at 366.1 °C, 359 °C, 357 °C and 364 °C, respectively. The results also indicated that CHBC had considerable thermostability.

3.3. Water absorbency and water retention capacity

As shown in Fig. 3(B), BC showed rapid water absorption capacity, and 50.25 ± 2.62 g/g water was absorbed into the BC structure in 2 h, while the total water absorbed by BC was 60.16 ± 3.64 g/g. The excellent water absorbency of BC could be attributed to the porous structure of BC and the large amount of hydroxyl groups on the surface of BC fibers [46]. The absorption rates of HBC, CBC and CHBC were 24.74 ± 2.03 g/g, 41.38 ± 2.93 g/g and 35.78 ± 2.45 g/g, respectively. The main reason for the decrease in the water absorption rate may be that the volume of BC did not increase after water absorption because of the rigid BC fiber. Therefore, the introduced Col-I and HACC occupied the pores of BC that would otherwise hold water. Furthermore, the absorption rate of CBC was higher than that of HBC, which may have been due to the high hydrophilicity of Col-I. Excellent water absorption is needed for an ideal dressing to remove the exuded fluid of the wound in time. The water absorption rates of Vaseline gauze, poly(1, 8-octanediol-cocitric acid)/polylactic acid electrospun nanofibrous membranes and tough chitosan dressings were 0.41 g/g, 7.6 g/g, and 21 g/g, respectively [42,47,48]. The water absorption rate of CHBC was significantly higher than that of the above three materials, which means that the absorption properties of CHBC can meet clinical needs.

The water retention rate of the samples is presented in Fig. 3(C). The water retention capacity of BC was very poor, and the water went within 10 h. Because the porosity of BC was higher than 89%, the hydroxyl groups on the BC fibers could hold only a small amount of water. The absorbed water in BC was mostly free water, which easily seeped out, as we observed. After introducing Col-I or HACC, CBC and HBC exhibited better water retention rates than BC. Notably, CHBC showed the best water retention capacity, and the water retention rate after 48 h was up to 11%. which may be attributed to the synergistic effect of Col-I and HACC.

3.4. WVTRs

The WVTRs of samples are shown in Fig. 3(D). BC exhibited a very high WVTR because of its hydrophilic nature, as reported in the literature [49]. The WVTR values of HBC (2922 ± 31 g m^{-2}·day^{-1}), CBC (2981 ± 46 g m^{-2}·day^{-1}) and CHBC (3084 ± 56 g m^{-2}·day^{-1}) were higher than that of BC (2819 ± 47 g m^{-2}·day^{-1}), and CHBC had the highest WVTR. The reason for this may be that the introduced Col-I or HACC could increase the space between the polymer chains, which could promote water vapor diffusivity through the sample [50]. The optimum WVTR of wound dressings varies from 1900 to 5800 g m^{-2}·day^{-1} [50]. Therefore, all of the BC-based dressings, especially CHBC, were suitable for wound dressings and maintained a moist environment, which could promote granulation growth and accelerate

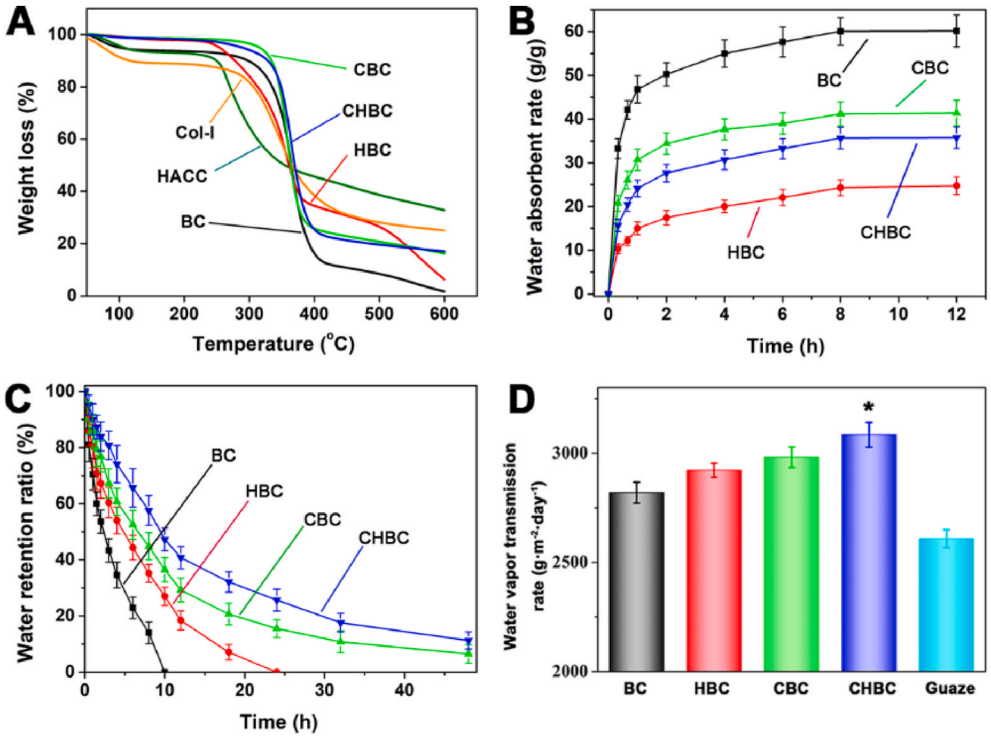

Fig. 3. Physicochemical properties of BC-based composite films, typical thermal degradation profiles (A), water absorption curves (B), water retention curves (C) and water vapor transmission rates (D). *$P < 0.05$ compared with Guaze.

wound healing.

3.5. Antibacterial properties

Although BC can protect against bacterial invention as a physical barrier, it does not have a bactericidal function and cannot clear existing infections, which may reduce its effectiveness for highly contaminated wounds [51]. In our previous work, the acceptable antibacterial properties of HACC/BC films were verified [29]. In this study, the effect of HACC and Col-I on the antimicrobial activity of CHBC was further investigated. The ZOI results shown in Fig. S2. There was no ZOI in the images of the BC and CBC groups, while the ZOIs of HBC and CHBC were obvious, indicating that HACC can be released to kill bacteria that did not come in contact with the material. It is worth noting that the ZOI of CHBC was slightly smaller than that of HBC (Fig. S2(B)). The reason for this may be that Col-I could promote bacterial growth, as well as human cell growth.

Fig. 4(A) shows the SEM images of colonizing bacteria at 6 h and biofilm formation at 24 h on different samples. After cultivation for 6 h, large amounts of bacteria colonized the surfaces of BC and CBC, while no bacteria were found on HBC and CHBC. After 24 h, the biofilms of *S. aureus* covered the surfaces of BC and CBC. In contrast, there were only a few bacteria in HBC and CHBC. The SEM results confirmed that BC-based composite films containing HACC could reduce the colonization and biofilm formation of *S. aureus*, and the effect of Col-I on antibacterial properties was minimal.

The condition of bacteria on the four kinds of samples was also observed by CLSM after staining with the LIVE/DEAD BacLight Bacterial Viability Kit (Fig. 4(B)). Whether cultivated for 6 h or 24 h, the bacteria on the surfaces of BC and CBC were green, indicating that they were alive. Most of the cells on the surface of HBCs and CHBCs were dead and stained red. The results of CLSM further demonstrated that BC-based composite films containing HACC could kill the bacteria colonizing the material and had favorable bactericidal functions, as reported in the literature [30].

3.6. Cytocompatibility

The proliferation of NIH-3T3 cells and HUVECs on the surfaces of BC-based composite films is shown in Fig. 5(A) and (B). Both cell lines proliferated very well on all specimens, and there was no evidence of cytotoxicity. The proliferation of cells in groups containing Col-I (CBC and CHBC) was distinctly better than that in the BC and HBC groups. Several studies reported that BC could suitably improve cell spreading and proliferation [11,52,53]. Nevertheless, the effect of BC on cells was based on the physical and chemical characteristics of BC, which were inferior to the biochemical signals of bioactive molecules [54–56]. Hyaluronan nanocomposites and silk scricin have been confirmed to

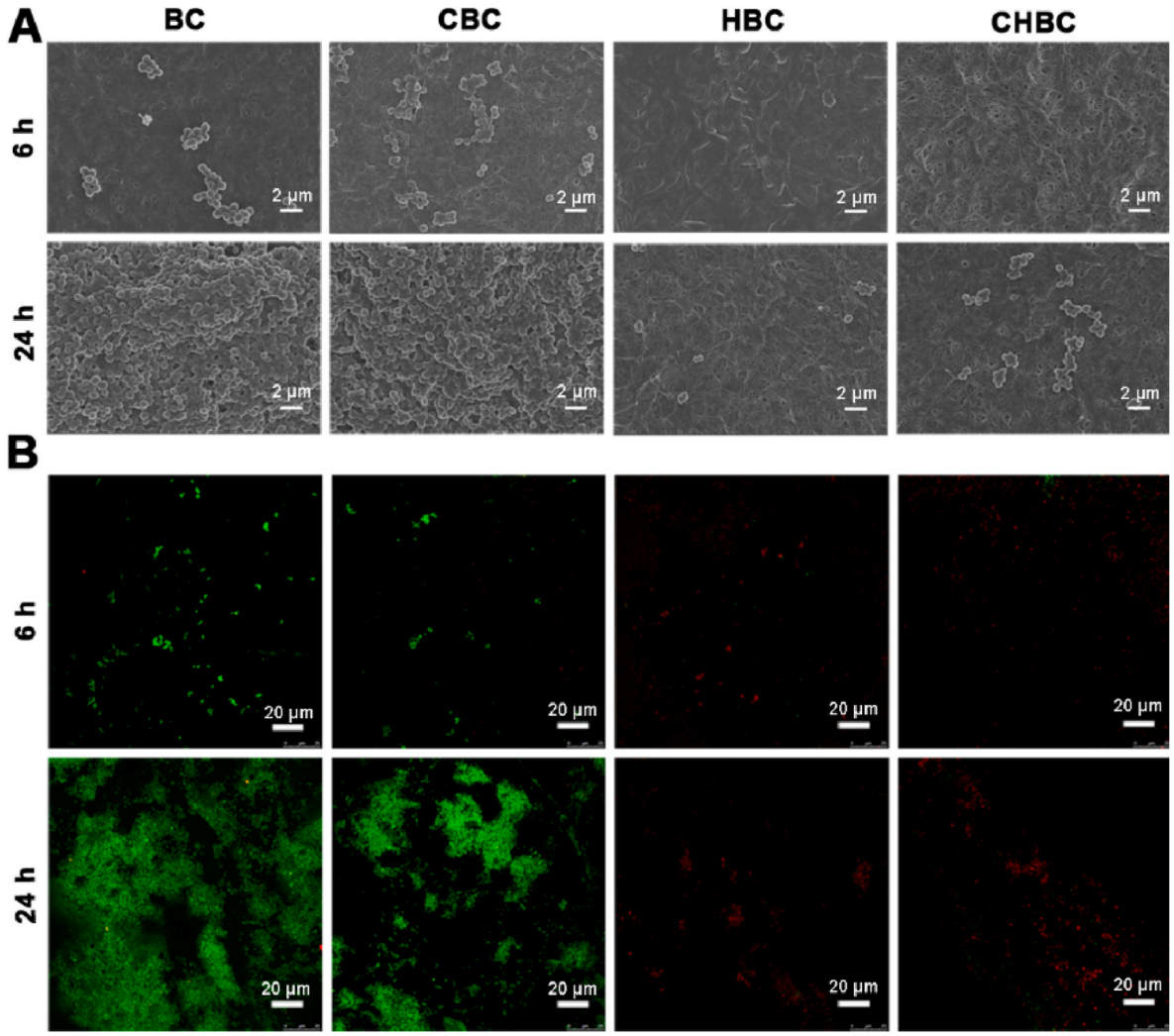

Fig. 4. Antibacterial properties of BC-based composite dressings and *S. aureus* were employed. (A) SEM images of colonized bacteria at 6 h and biofilm formation at 24 h on different samples; (B) CLSM images of living bacteria (green) and dead bacteria (red) on different samples after the Live/dead bacteria staining at 6 h and 24 h.

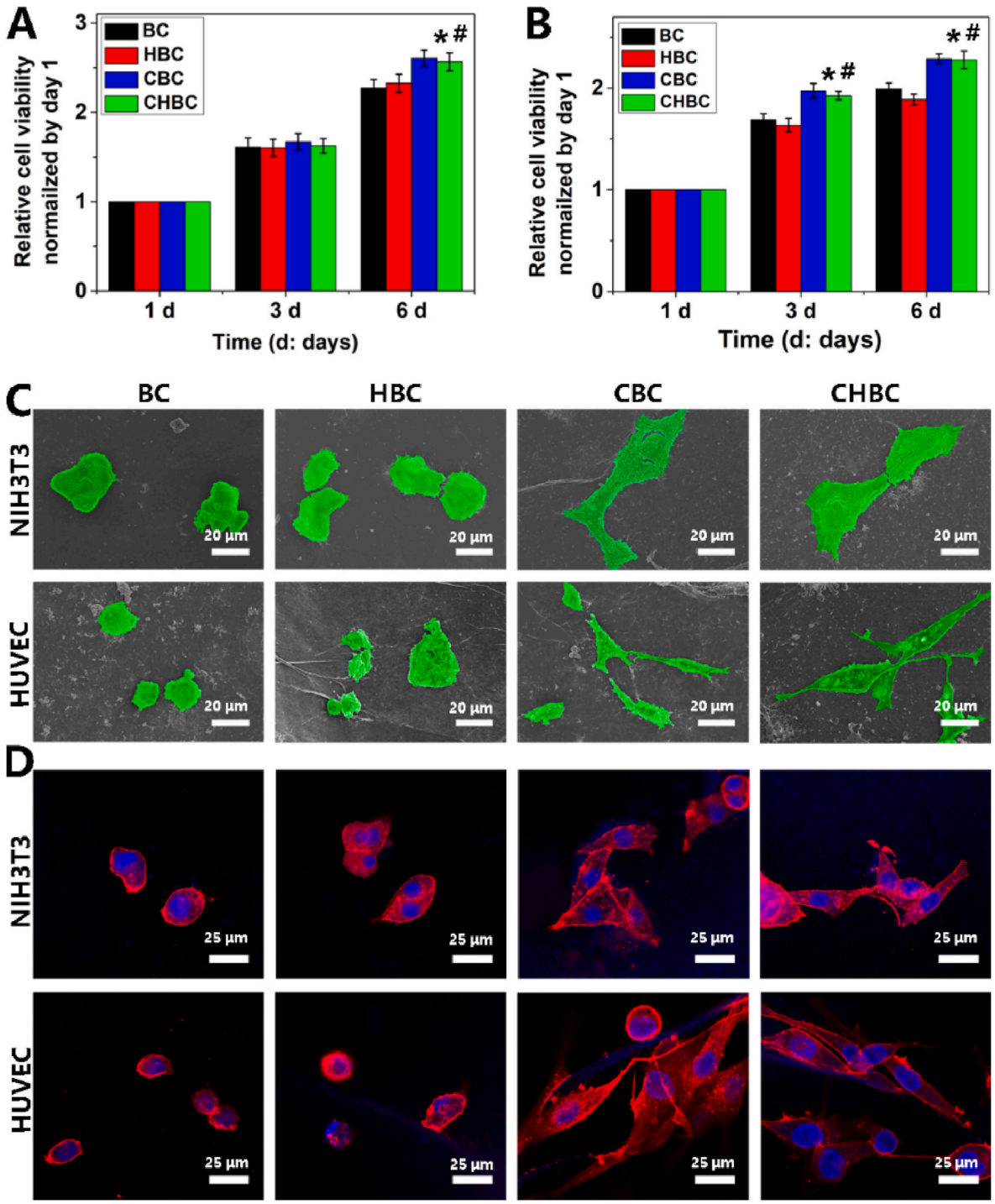

Fig. 5. Cytocompatibility of BC-based composite dressings. (A) and (B) show the relative proliferation rates of NIH3T3 cells (A) and HUVECs (B) on different samples; (C) shows SEM morphologies of cells on samples; (D) shows the cytoskeletal morphology and spreading of cells on samples. $^{*}P < 0.05$ compared CHBC with BC and HBC, $^{\#}P > 0.05$ compared CHBC with CBC.

improve the cytocompatibility of BC, as well as Col-I employed in this work [57,58]. It is worth noting that there was no significant difference between CBC and CHBC, indicating that the antibacterial agent HACC had no effect on the cytocompatibility of CHBC.

To further verify the cytocompatibility of CHBCs, images of NIH-3T3 cells and HUVECs on specimens after cultivation for 3 days were observed by SEM and CLSM, and the results are shown in Fig. 5(C) and (D). Cells on CBC and CHBC showed complete spread and exhibited a polygonal and fusiform morphology, while those on BC and HBC retained their original appearance because of incomplete spread. The results indicated that CHBCs had excellent cytocompatibility, which was conferred by Col-I.

3.7. *In vivo* wound healing

Inhibiting infection and promoting healing are two important properties of ideal wound dressings. In *in vivo* studies, a wound infection model was established to detect the ability of the CHBC functional dressing to treat infected wounds. The macrolevel observation of the healing process is shown in Fig. 6(A). On day 2, obvious suppuration was

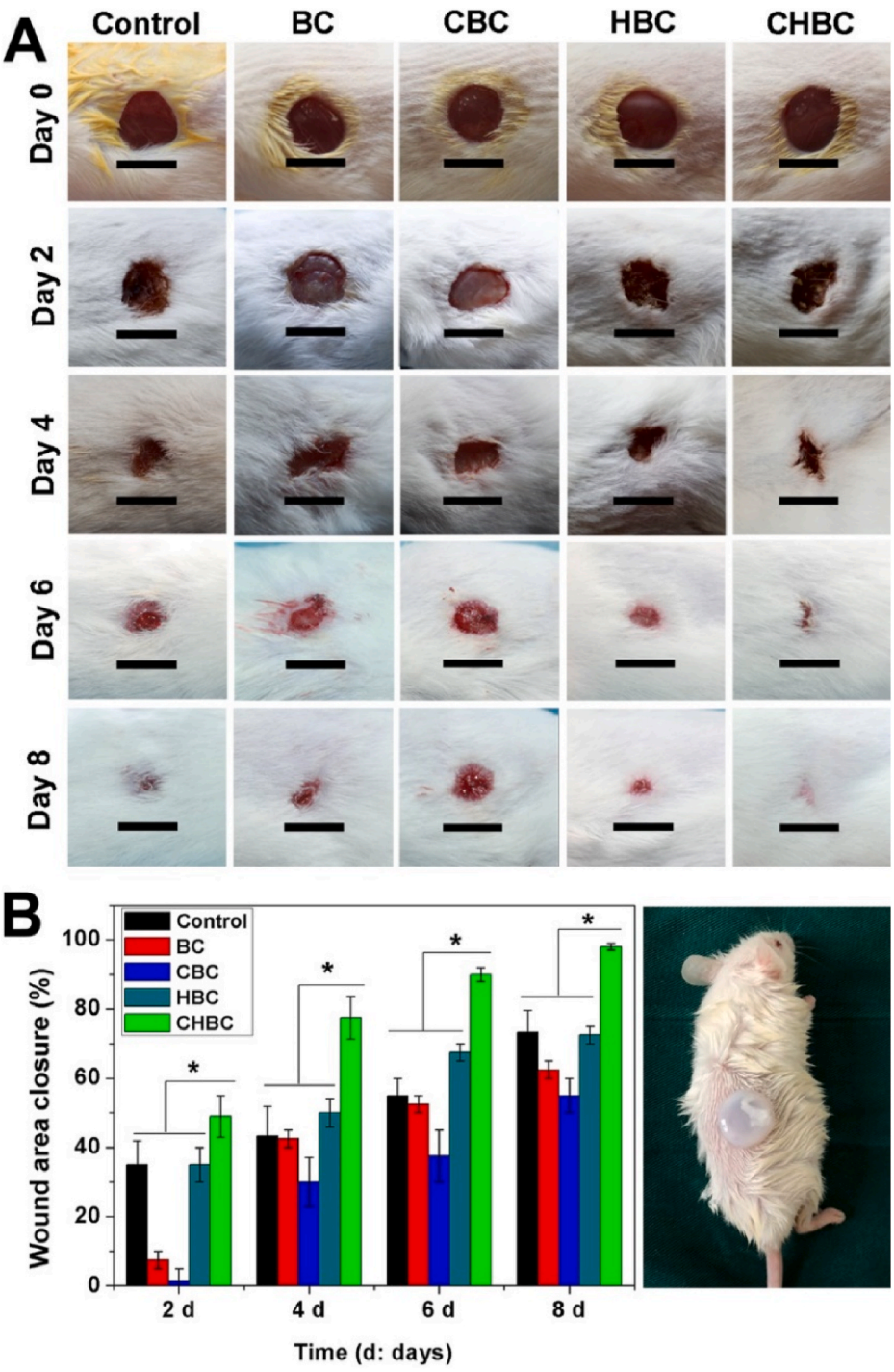

Fig. 6. *In vivo* animal experiment results. (A) Representative photographs of the wounds on Day 0, 2, 4, 6 and 8 after covering with dressing. The wounds without infection and treated with BC were noted in the control group. The bar was 10 mm. (B) is wound area closure percentage of wounds. *$P < 0.05$ compared CHBC group with other groups.

observed in the BC group, while there were no signs of infection in the control group, indicating that the wound infection model was established successfully. The same symptoms of infection occurred in the CBC group but not in the HBC and CHBC groups. The infection in the BC and CBC groups was also verified by SEM of wound tissue on day 2 (Fig. S3). The tissue surface of the control, HBC and CHBC groups was smooth without any trace of damage. However, a large number of pores formed by bacteria were found on the surface of the BC and CBC specimens. The results indicated that the antibacterial agent HACC could prevent infections caused by gram-positive bacteria. Similar results have been reported in our previous studies [27,30,59].

Throughout the healing process, the healing effect of the BC group was worse than that of the control group, which was attributed to the infection. Unfortunately, after Col-I was introduced, the healing of infected wounds in the CBC group was slower than that in the BC group, which may be because Col-I could promote bacterial growth. The results indicated that Col-I alone has a negative effect on infectious cutaneous wound healing. As expected, the wounds of the HBC group healed better than those of the BC group because of the elimination of infection, as described in the literature [21]. It was exciting that the fastest healing

process occurred in the CHBC group. Almost all wounds healed, the skin approached a normal appearance on day 8, and robust hair growth was noted. These results may be due to the synergy of collagen and HACC. HACC cleared bacteria to prevent infection, while Col-I promoted cell growth and tissue healing. The RC of the wound area was statistically analyzed and is shown in Fig. 6(B). Wound healing in the BC and CBC groups was severely delayed by bacterial infection, and the RC values of the BC and CBC groups on day 2 were only 6.5 ± 4.5% and 3.3 ± 2.7%, respectively, which were much lower than those of the control (39.1 ± 3.7%), HBC (41.8 ± 3.3%) and CHBC (53.2 ± 3.1%) groups. The RC of the CHBC group at all time points was significantly higher than that of the other groups. After 8 days of treatment, the RC of the CHBC group was almost 100%, which was clearly higher than that of the control (81.1 ± 2.0%), BC (72.3 ± 2.6%), CBC (55.5 ± 3.1%) and HBC (72.5 ± 2.5%) groups. Several studies have also reported that the healing time of infected wounds treated with antibacterial dressings was approximately 2 weeks [60–63].

To evaluate wound healing and tissue regeneration at the histological level, H&E staining was employed, and the results are shown in Fig. 7(A). On day 4, the epithelial tissue of the BC and CBC groups showed a large number of scattered inflammatory cells. The results indicated that infected wounds (BC and CBC groups) were more difficult to heal than normal wounds (control group), even though CBCs contained collagen. In contrast, the epithelial tissue of the HBC and CHBC groups grew neatly, with fewer inflammatory cells, and new hair follicles (blue arrow) were formed, which, due to the infection, were eliminated by HACC, allowing the wound to heal normally. Interestingly, more regular new tissue and new hair follicles were observed in the CHBC group than in the HBC group at both time points.

In the process of wound healing, collagen synthesized by fibroblasts is the main component of the extracellular matrix, so the deposition of collagen at the wound site is of great significance for wound repair [64]. Masson's trichrome staining was used to evaluate the expression of collagen in the wound at different time points, and the results are shown in Fig. 7(B). Collagen deposition in the BC and CBC groups was lower than that in the other three groups at both time points because of infection. Unfortunately, the CBC group showed the lowest collagen expression, which may be due to the aggravation of infection and worse wound healing caused by the introduction of collagen alone. Interestingly, collagen deposition was highest in the CHBC group, and collagen was evenly distributed in each part of the epidermis and dermis. The results further indicated that CHBCs could promote the deposition of collagen around the wound and inhibit the growth of bacteria to prevent wound infection, leading to better wound healing.

4. Conclusions

In summary, a CHBC composite film was fabricated successfully as a novel multifunctional wound dressing *via* MLI culture. The CHBC dressings showed a porous structure and good water absorption, which are conducive to the absorption of exudates around the wound and the maintenance of a moist environment. Furthermore, the CHBC dressings exhibited favorable antibacterial properties against *S. aureus* and good cytocompatibility to promote NIH3T3 cell and HUVEC proliferation and spread. Most importantly, the CHBC dressings significantly prevented wound infection, reduced inflammation, promoted wound healing, and accelerated the formation of new epithelial tissue compared with BC. These favorable multifunctional properties suggest that CHBC dressings have great potential for treating infected wounds.

CRediT authorship contribution statement

Chen Zhou: Conceptualization, Investigation, Writing – original draft, Formal analysis. **Zhifei Yang:** Investigation. **Xiaowei Xun:**

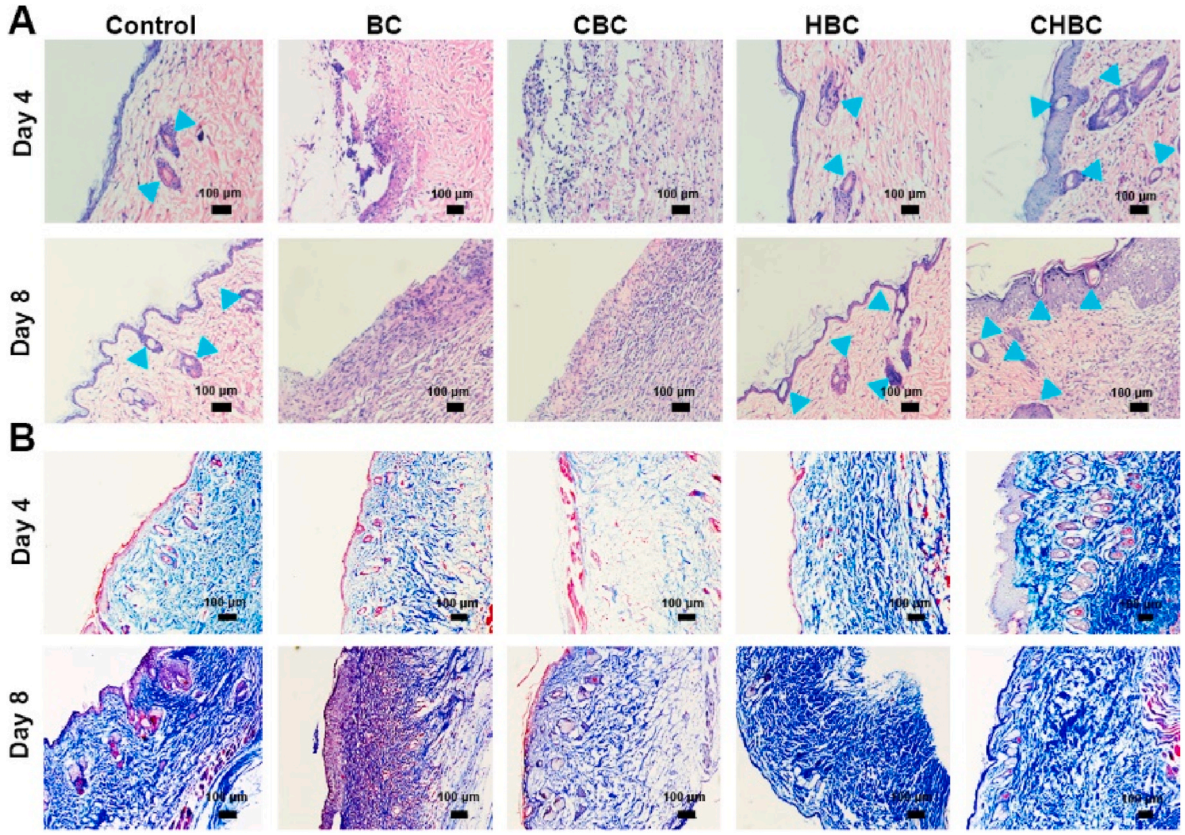

Fig. 7. Histological assessment of wound area on day 4 and day 8 postsurgery. (A) H&E staining, the blue arrow indicates new hair follicles; (B) Masson's trichrome staining. The bar was 100 μm.

Investigation. **Le Ma:** Data curation. **Zejing Chen:** Writing – review & editing. **Xiaoming Hu:** Writing – review & editing. **Xidong Wu:** Writing – review & editing. **Yizao Wan:** Funding acquisition, Supervision. **Haiyong Ao:** Conceptualization, Funding acquisition, Resources, Writing – original draft, Writing – review & editing, Project administration.

Declaration of competing interest

The authors declare that they have no known competing financial interests or personal relationships that could have appeared to influence the work reported in this paper.

Acknowledgements

This work is supported by the National Natural Science Foundation of China (Grant No. 31760265 and 82160355), grant awarded by Natural Science Foundation of Jiangxi Province (20171ACB21036 and 20192ACB80008).

Appendix A. Supplementary data

Supplementary data to this article can be found online at https://doi.org/10.1016/j.bioactmat.2021.10.043.

References

[1] P.R.F.d.S. Moraes, S. Saska, H. Barud, L.R.d. Lima, V.d.C.A. Martins, A.M.d. G. Plepis, S.J.L. Ribeiro, A.M.M. Gaspar, Bacterial cellulose/collagen hydrogel for wound healing, Mater. Res. 19 (2016) 106–116.
[2] D.N. Herndon, R.E. Barrow, R.L. Rutan, T.C. Rutan, M.H. Desai, S. Abston, A comparison of conservative versus early excision. Therapies in severely burned patients, Ann. Surg. 209 (1989) 547–552.
[3] Y. Li, S. Wang, R. Huang, Z. Huang, B. Hu, W. Zheng, G. Yang, X. Jiang, Evaluation of the effect of the structure of bacterial cellulose on full thickness skin wound repair on a microfluidic chip, Biomacromolecules 16 (2015) 780–789.
[4] W. Czaja, A. Krystynowicz, S. Bielecki, R. Brownjr, Microbial cellulose—the natural power to heal wounds, Biomaterials 27 (2006) 145–151.
[5] Z. Cao, X. Luo, H. Zhang, Z. Fu, Z. Shen, N. Cai, Y. Xue, F. Yu, A facile and green strategy for the preparation of porous chitosan-coated cellulose composite membranes for potential applications as wound dressing, Cellulose 23 (2016) 1349–1361.
[6] Y. Qiu, L. Qiu, J. Cui, Q. Wei, Bacterial cellulose and bacterial cellulose-vaccarin membranes for wound healing, Mater. Sci. Eng. C 59 (2016) 303–309.
[7] J.D. Fontana, A.M. de Souza, C.K. Fontana, I.L. Torriani, J.C. Moreschi, B. J. Gallotti, S.J. de Souza, G.P. Narcisco, J.A. Bichara, L.F. Farah, Acetobacter cellulose pellicle as a temporary skin substitute, Appl. Biochem. Biotechnol. 24–25 (1990) 253–264.
[8] A. Żywicka, K. Fijałkowski, A.F. Junka, J. Grzesiak, M. El Fray, Modification of bacterial cellulose with quaternary ammonium compounds based on fatty acids and amino acids and the effect on antimicrobial activity, Biomacromolecules 19 (2018) 1528–1538.
[9] Y. Li, H. Jiang, W. Zheng, N. Gong, L. Chen, X. Jiang, G. Yang, Bacterial cellulose–hyaluronan nanocomposite biomaterials as wound dressings for severe skin injury repair, J. Mater. Chem. B 3 (2015) 3498–3507.
[10] F. Feizabadi, M. Minaiyan, A. Taheri, Arginine functionalized bacterial cellulose nanofibers containing gel as an effective wound dressing: in vitro and in vivo evaluation, Curr. Drug Deliv. 15 (2018) 840–849.
[11] H. Qiao, T. Guo, Y. Zheng, L. Zhao, Y. Sun, Y. Liu, Y. Xie, A novel microporous oxidized bacterial cellulose/arginine composite and its effect on behavior of fibroblast/endothelial cell, Carbohydr. Polym. 184 (2018) 323–332.
[12] C.N. Wu, S.C. Fuh, S.P. Lin, Y.Y. Lin, H.Y. Chen, J.M. Liu, K.C. Cheng, TEMPO-oxidized bacterial cellulose pellicle with silver nanoparticles for wound dressing, Biomacromolecules 19 (2018) 544–554.
[13] M.J. Tabaii, G. Emtiazi, Transparent nontoxic antibacterial wound dressing based on silver nano, J. Drug Deliv. Sci. Technol. 44 (2018) 244–253.
[14] E. Altun, M.O. Aydogdu, M. Crabbe-Mann, J. Ahmed, F. Brako, B. Karademir, B. Aksu, M. Sennaroglu, M.S. Eroglu, G. Ren, O. Gunduz, M. Edirisinghe, Co-Culture of keratinocyte-*Staphylococcus aureus* on Cu-Ag-Zn/CuO and Cu-Ag-W nanoparticle loaded bacterial cellulose: PMMA bandages, Macromol. Mater. Eng. 304 (2019) 1800537.
[15] S. Adepu, M. Khandelwal, Broad-spectrum antimicrobial activity of bacterial cellulose silver nanocomposites with sustained release, J. Mater. Sci. 53 (2017) 1596–1609.
[16] M. Fursatz, M. Skog, P. Sivler, E. Palm, C. Aronsson, A. Skallberg, G. Greczynski, H. Khalaf, T. Bengtsson, D. Aili, Functionalization of bacterial cellulose wound dressings with the antimicrobial peptide epsilon-poly-L-Lysine, Biomed. Mater. 13 (2018), 025014.
[17] S. Jiji, S. Udhayakumar, C. Rose, C. Muralidharan, K. Kadirvelu, Thymol enriched bacterial cellulose hydrogel as effective material for third degree burn wound repair, Int. J. Biol. Macromol. 122 (2019) 452–460.
[18] D. Zmejkoski, D. Spasojevic, I. Orlovska, N. Kozyrovska, M. Sokovic, J. Glamoclija, S. Dmitrovic, B. Matovic, N. Tasic, V. Maksimovic, M. Sosnin, K. Radotic, Bacterial cellulose-lignin composite hydrogel as a promising agent in chronic wound healing, Int. J. Biol. Macromol. 118 (2018) 494–503.
[19] B. Sun, Y. Zhang, W. Li, X. Xu, H. Zhang, Y. Zhao, J. Lin, D. Sun, Facile synthesis and light-induced antibacterial activity of ketoprofen functionalized bacterial cellulose membranes, Colloid. Surface. 568 (2019) 231–238.
[20] C. Chuah, J. Wang, J. Tavakoli, Y. Tang, Novel bacterial cellulose-poly (acrylic acid) hybrid hydrogels with controllable antimicrobial ability as dressings for chronic wounds, Polymers 10 (2018) 1323.
[21] S. Ye, L. Jiang, J. Wu, C. Su, C. Huang, X. Liu, W. Shao, Flexible amoxicillin-grafted bacterial cellulose sponges for wound dressing: in vitro and in vivo evaluation, ACS Appl. Mater. Interfaces 10 (2018) 5862–5870.
[22] Y. Xie, L. Yue, Y. Zheng, L. Zhao, C. Liang, W. He, Z. Liu, Y. Sun, Y. Yang, The antibacterial stability of poly(dopamine) in-situ reduction and chelation nano-Ag based on bacterial cellulose network template, Appl. Surf. Sci. 491 (2019) 383–394.
[23] S.R.Z. Teixeira, E.M.d. Reis, G.P. Apati, M.M. Meier, A.L. Nogueira, M.C.F. Garcia, A.L.d.S. Schneider, A.P.T. Pezzin, L.M. Porto, Biosynthesis and functionalization of bacterial cellulose membranes with cerium nitrate and silver nanoparticles, Mater. Res. 22 (2019), e20190054.
[24] L.M.P. Sampaio, J. Padrão, J. Faria, J.P. Silva, C.J. Silva, F. Dourado, A. Zille, Laccase immobilization on bacterial nanocellulose membranes: antimicrobial, kinetic and stability properties, Carbohydr. Polym. 145 (2016) 1–12.
[25] Z.X. Peng, L. Wang, L. Du, S.R. Guo, X.Q. Wang, T.T. Tang, Adjustment of the antibacterial activity and biocompatibility of hydroxypropyltrimethyl ammonium chloride chitosan by varying the degree of substitution of quaternary ammonium, Carbohydr. Polym. 81 (2010) 275–283.
[26] H. Tan, S. Guo, S. Yang, X. Xu, T. Tang, Physical characterization and osteogenic activity of the quaternized chitosan-loaded PMMA bone cement, Acta Biomater. 8 (2012) 2166–2174.
[27] Z. Peng, H. Ao, L. Wang, S. Guo, T. Tang, Quaternised chitosan coating on titanium provides a self-protective surface that prevents bacterial colonisation and implant-associated infections, RSC Adv. 5 (2015) 54304–54311.
[28] Y. Yang, H.Y. Ao, Y.G. Wang, W.T. Lin, S.B. Yang, S.H. Zhang, Z.F. Yu, T.T. Tang, Cytocompatibility with osteogenic cells and enhanced in vivo anti-infection potential of quaternized chitosan-loaded titania nanotubes, Bone Res 4 (2016) 16027.
[29] H. Ao, W. Jiang, Y. Nie, C. Zhou, J. Zong, M. Liu, X. Liu, Y. Wan, Engineering quaternized chitosan in the 3D bacterial cellulose structure for antibacterial wound dressings, Polym. Test. 86 (2020) 106490.
[30] H. Ao, S. Yang, B.e. Nie, Q. Fan, Q. Zhang, J. Zong, S. Guo, X. Zheng, T. Tang, Improved antibacterial properties of collagen I/hyaluronic acid/quaternized chitosan multilayer modified titanium coatings with both contact-killing and release-killing functions, J. Mater. Chem. B 7 (2019) 1951–1961.
[31] H. Luo, H. Ao, M. Peng, F. Yao, Z. Yang, Y. Wan, Effect of highly dispersed graphene and graphene oxide in 3D nanofibrous bacterial cellulose scaffold on cell responses: a comparative study, Mater. Chem. Phys. 235 (2019) 121774.
[32] H. Luo, P. Xiong, J. Xie, Z. Yang, Y. Huang, J. Hu, Y. Wan, Y. Xu, Uniformly dispersed freestanding carbon nanofiber/graphene electrodes made by a scalable biological method for high-performance flexible supercapacitors, Adv. Funct. Mater. 28 (2018) 1803075.
[33] L. Segal, J.J. Creely, A.E. Martin, C.M. Conrad, An empirical method for estimating the degree of crystallinity of native cellulose using the X-ray diffractometer, Textil. Res. J. 29 (1959) 786–794.
[34] S. Jiji, S. Udhayakumar, K. Maharajan, C. Rose, C. Muralidharan, K. Kadirvelu, Bacterial cellulose matrix with in situ impregnation of silver nanoparticles via catecholic redox chemistry for third degree burn wound healing, Carbohydr. Polym. 245 (2020) 116573.
[35] B.E. Nie, H. Ao, C. Chen, K. Xie, J. Zhou, T. Long, T. Tang, B. Yue, Covalent immobilization of KR-12 peptide onto a titanium surface for decreasing infection and promoting osteogenic differentiation, RSC Adv. 6 (2016) 46733–46743.
[36] H. Ao, Y. Xie, H. Tan, S. Yang, K. Li, X. Wu, X. Zheng, T. Tang, Fabrication and in vitro evaluation of stable collagen/hyaluronic acid biomimetic multilayer on titanium coatings, J. R. Soc. Interface 10 (2013) 20130070.
[37] M. Yang, J. Ward, K.L. Choy, Nature-inspired bacterial cellulose/methylglyoxal (BC/MGO) nanocomposite for broad-spectrum antimicrobial wound dressing, Macromol. Biosci. 20 (2020) 2000070.
[38] M.L. Cacicedo, G. Pacheco, G.A. Islan, V.A. Alvarez, H.S. Barud, G.R. Castro, Chitosan-bacterial cellulose patch of ciprofloxacin for wound dressing: preparation and characterization studies, Int. J. Biol. Macromol. 147 (2020) 1136–1145.
[39] H. Ao, Y. Xie, H. Tan, X. Wu, G. Liu, A. Qin, X. Zheng, T. Tang, Improved hMSC functions on titanium coatings by type I collagen immobilization, J. Biomed. Mater. Res. 102 (2014) 204–214.
[40] Z. Cai, J. Kim, Bacterial cellulose/poly(ethylene glycol) composite: characterization and first evaluation of biocompatibility, Cellulose 17 (2009) 83–91.
[41] H. Luo, J. Dong, X. Xu, J. Wang, Z. Yang, Y. Wan, Exploring excellent dispersion of graphene nanosheets in three-dimensional bacterial cellulose for ultra-strong nanocomposite hydrogels, Compos Part A: Appl Sci 109 (2018) 290–297.
[42] H. Luo, J. Dong, Y. Zhang, G. Li, R. Guo, G. Zuo, M. Ye, Z. Wang, Z. Yang, Y. Wan, Constructing 3D bacterial cellulose/graphene/polyaniline nanocomposites by

novel layer-by-layer in situ culture toward mechanically robust and highly flexible freestanding electrodes for supercapacitors, Chem. Eng. J. 334 (2018) 1148–1158.
[43] D.T.B. De Salvi, H.S. Barud, J.M.A. Caiut, Y. Messaddeq, S.J.L. Ribeiro, Self-supported bacterial cellulose/boehmite organic-inorganic hybrid films, J. Sol. Gel Sci. Technol. 63 (2012) 211–218.
[44] H.G. Oliveira Barud, H.d.S. Barud, M. Cavicchioli, T.S. do Amaral, O.B.d.O. Junior, D.M. Santos, A.L.d.O.A. Petersen, F. Celes, V.M. Borges, C.I. de Oliveira, P.F. de Oliveira, R.A. Furtado, D.C. Tavares, S.J.L. Ribeiro, Preparation and characterization of a bacterial cellulose/silk fibroin sponge scaffold for tissue regeneration, Carbohydr. Polym. 128 (2015) 41–51.
[45] N.F. Vasconcelos, F.K. Andrade, L.d.A.P. Vieira, R.S. Vieira, J.M. Vaz, P. Chevallier, D. Mantovani, M.d.F. Borges, M.d.F. Rosa, Oxidized bacterial cellulose membrane as support for enzyme immobilization: properties and morphological features, Cellulose 27 (2020) 3055–3083.
[46] N. Eslahi, A. Mahmoodi, N. Mahmoudi, N. Zandi, A. Simchi, Processing and properties of nanofibrous bacterial cellulose-containing polymer composites: a review of recent advances for biomedical applications, Polym. Rev. 60 (2019) 144–170.
[47] F. Zou, X. Sun, X. Wang, Elastic, hydrophilic and biodegradable poly (1, 8-octanediol-co-citric acid)/polylactic acid nanofibrous membranes for potential wound dressing applications, Polym. Degrad. Stabil. 166 (2019) 163–173.
[48] Y. Kong, X. Tang, Y. Zhao, X. Chen, K. Yao, L. Zhang, Q. Han, L. Zhang, J. Ling, Y. Wang, Y. Yang, Degradable tough chitosan dressing for skin wound recovery, Nanotechnol. Rev. 9 (2020) 1576–1585.
[49] Z. Luo, J. Liu, H. Lin, X. Ren, H. Tian, Y. Liang, W. Wang, Y. Wang, M. Yin, Y. Huang, J. Zhang, In situ fabrication of nano ZnO/BCM biocomposite based on MA modified bacterial cellulose Membrane for antibacterial and wound healing, Int. J. Nanomed. 15 (2020) 1–15.
[50] Y. Wang, C. Wang, Y. Xie, Y. Yang, Y. Zheng, H. Meng, W. He, K. Qiao, Highly transparent, highly flexible composite membrane with multiple antimicrobial effects used for promoting wound healing, Carbohydr. Polym. 222 (2019) 114985.
[51] I. Sulaeva, U. Henniges, T. Rosenau, A. Potthast, Bacterial cellulose as a material for wound treatment: properties and modifications, A review, Biotechnol Adv 33 (2015) 1547–1571.
[52] S.H. Lee, Y.M. Lim, S.I. Jeong, S.J. An, S.S. Kang, C.M. Jeong, J.B. Huh, The effect of bacterial cellulose membrane compared with collagen membrane on guided bone regeneration, J Adv Prosthodont 7 (2015) 484.
[53] Y. Wan, S. Yang, J. Wang, D. Gan, M. Gama, Z. Yang, Y. Zhu, F. Yao, H. Luo, Scalable synthesis of robust and stretchable composite wound dressings by dispersing silver nanowires in continuous bacterial cellulose, Compos. B Eng. 199 (2020) 108259.
[54] G. Helenius, H. Backdahl, A. Bodin, U. Nannmark, P. Gatenholm, B. Risberg, In vivo biocompatibility of bacterial cellulose, J. Biomed. Mater. Res. 76A (2006) 431–438.
[55] M. Zaborowska, A. Bodin, H. Bäckdahl, J. Popp, A. Goldstein, P. Gatenholm, Microporous bacterial cellulose as a potential scaffold for bone regeneration, Acta Biomater. 6 (2010) 2540–2547.
[56] R.A.N. Pertile, F.K. Andrade, C. Alves Jr., M. Gama, Surface modification of bacterial cellulose by nitrogen-containing plasma for improved interaction with cells, Carbohydr. Polym. 82 (2010) 692–698.
[57] Y. Li, H. Jiang, W.F. Zheng, N.Y. Gong, L.L. Chen, X.Y. Jiang, G. Yang, Bacterial cellulose-hyaluronan nanocomposite biomaterials as wound dressings for severe skin injury repair, J. Mater. Chem. B 3 (2015) 3498–3507.
[58] L. Lamboni, Y. Li, J. Liu, G. Yang, Silk sericin-functionalized bacterial cellulose as a potential wound-healing biomaterial, Biomacromolecules 17 (2016) 3076–3084.
[59] H.L. Tan, H.Y. Ao, R. Ma, W.T. Lin, T.T. Tang, In vivo effect of quaternized chitosan-loaded polymethylmethacrylate bone cement on methicillin-resistant *Staphylococcus epidermidis* infection of the tibial metaphysis in a rabbit model, Antimicrob Agents Ch 58 (2014) 6016–6023.
[60] X. Zhao, H. Wu, B. Guo, R. Dong, Y. Qiu, P.X. Ma, Antibacterial anti-oxidant electroactive injectable hydrogel as self-healing wound dressing with hemostasis and adhesiveness for cutaneous wound healing, Biomaterials 122 (2017) 34–47.
[61] J. Qu, X. Zhao, Y. Liang, T. Zhang, P.X. Ma, B. Guo, Antibacterial adhesive injectable hydrogels with rapid self-healing, extensibility and compressibility as wound dressing for joints skin wound healing, Biomaterials 183 (2018) 185–199.
[62] J. He, M. Shi, Y. Liang, B. Guo, Conductive adhesive self-healing nanocomposite hydrogel wound dressing for photothermal therapy of infected full-thickness skin wounds, Chem. Eng. J. 394 (2020) 124888.
[63] M. Zare-Gachi, H. Daemi, J. Mohammadi, P. Baei, F. Bazgir, S. Hosseini-Salekdeh, H. Baharvand, Improving anti-hemolytic, antibacterial and wound healing properties of alginate fibrous wound dressings by exchanging counter-cation for infected full-thickness skin wounds, Mater. Sci. Eng. C 107 (2020) 110321.
[64] J. Peng, H. Zhao, C. Tu, Z. Xu, L. Ye, L. Zhao, Z. Gu, D. Zhao, J. Zhang, Z. Feng, In situ hydrogel dressing loaded with heparin and basic fibroblast growth factor for accelerating wound healing in rat, Mater. Sci. Eng. C 116 (2020) 111169.